Meteorol. Atmos. Phys. 46, 41–50 (1991)

Meteorology and Atmospheric Physics

551.576

University of Utah, Department of Meteorology/CARSS, Salt Lake City, Utah 84112, U.S.A.

Ice Cloud Microphysics, Radiative Transfer and Large-Scale Cloud Processes

K. N. Liou, J. L. Lee, S. C. Ou, Q. Fu and **Y. Takano**

With 7 Figures

Received September 7, 1990
Revised January 31, 1991

Summary

Parameterization programs for cloud microphysics and radiative transfer involving ice clouds have been developed in terms of the mean effective size and ice water path. The mean effective size appears to be adequate in representing the ice crystal size distribution for radiative parameterizations. For a given ice water path, smaller mean effective sizes reflect more solar radiation, emit more IR radiation and enhance net radiative heating/cooling at the cloud top and bottom than larger sizes. The presence of small ice crystals may generate steeper lapse rates in clouds. A 3-D global cloud model that prescribes the horizontal wind fields in a 24 hour period is used to investigate the sensitivity of the mean effective size of ice crystals on the simulation of radiative heating, temperature, cloud cover and ice water content. A variation in the mean effective size from 75 to 50 μm in a 24 hour prediction simulation generates more cooling above the high cloud top and a decrease of temperature. These results lead to an increase of high cloud cover in some latitudes by as much as 4% and, at the same time, a decrease of middle cloud cover by 3–4% in latitudes between 60°S and 60°N.

1. Introduction

In recognition of the importance of the role of clouds in weather and climate processes, numerous efforts have been made to include a more realistic and physically based parameterization for cloud parameters in general circulation models (Sundqvist, 1988; Liou and Zheng, 1984; Heymsfield and Donner, 1990; Smith, 1990). To understand the effects and feedbacks of clouds on dynamic and thermodynamic systems, the microphysical processes that govern the formation and dissipation of clouds must be adequately incorporated in atmospheric models. Furthermore, the radiative properties of clouds are determined by the cloud thermodynamic phase (ice or water), particle size distribution and geometric configuration. It appears to be impractical to include individual cloud particles in cloud models and radiation calculations. We must rely on some aspect of the cloud particle size distribution in the performance of radiation parameterizations in numerical models.

In this paper, we explore the means by which cloud microphysics and radiative transfer can be effectively and physically parameterized for incorporation in large-scale cloud and atmospheric models. We shall confine our presentation to high clouds that contain ice particles. In Sections 2 and 3, we present parameterization programs for cloud microphysics and radiative transfer in clouds, respectively. The mean effective size is proposed to represent ice crystal size distribution in radiation parameterizations. In Section 4, we investigate the sensitivity of mean effective size to the simulation of radiative heating, temperature, cloud cover and ice water content (IWC) using the global cloud model developed by Lee et al. (1990). Finally, conclusions are given in Section 5.

2. Parameterization of Cloud Microphysics

It is not computationally feasible to account for individual cloud particles in radiative transfer calculations. Nor is it practical to incorporate a program that takes into account the growth of individual water droplets and ice crystals in cloud models. However, some measure of the particle size distribution may be used. From the perspective of radiation calculations, particles scatter an amount of light proportionate to their cross-section area. The cross-section of a nonspherical particle is proportional to the maximum dimension (or the length, L) multiplied by the width, D. Thus, we may define a mean effective width (size) for hexagonal ice crystals in the form

$$D_e = \int_{L_{min}}^{L_{max}} D \cdot LD\, n(L) dL \Big/ \int_{L_{min}}^{L_{max}} LD\, n(L) dL, \qquad (1)$$

where L_{min} and L_{max} denote the limits of the ice crystal length. From laboratory and aircraft observations (Auer and Veal, 1970; Heymsfield, 1972; Hobb et al., 1974), the width of an ice particle can be related to the length via the following equation: $D = a_1 L^{b_1}$, where a_1 and b_1 are certain coefficients that are dependent on the particle shape.

The ice water content is defined by

$$\mathrm{IWC} = \int_{L_{min}}^{L_{max}} m(L)\, n(L) dL, \qquad (2)$$

where the mass of an individual ice crystal may be related to the length (Heymsfield, 1972): $m = a_2 L^{b_2}$, with a_2 and b_2 being certain coefficients. From Eqs. (1) and (2), IWC and D_e may be related through the ice crystal size distribution. The vertical IWC or ice water path (IWP) for a given thickness, Δz, is

$$\mathrm{IWP} = \mathrm{IWC} \cdot \Delta z. \qquad (3)$$

The other cloud physics parameter that is critically dependent on ice crystal size distribution is the bulk terminal velocity, which is defined by

$$V_T = \int_{L_{min}}^{L_{max}} n(L)\, m(L)\, v(L) dL \Big/ \int_{L_{min}}^{L_{max}} n(L)\, m(L) dL, \qquad (4)$$

where v is the terminal velocity for an individual ice crystal, which can be determined by the crystal length based on laboratory results (Jayaweera and Cottis, 1969; Heymsfield, 1972). Thus we have: $v = a_3 L^{b_3}$, with a_3 and b_3 being certain coefficients (Starr and Cox, 1985).

The ice crystal size distribution for midlatitude cirrus clouds has been measured by Heymsfield (1977) using an optical probe. Based on the measured data, Heymsfield and Platt (1984) grouped the size distributions according to temperatures ranging from -20 to -60°C and proposed a parameterized equation in the form

$$n(L) = A\, L^B, \qquad (5)$$

where both coefficients A and B are dependent on temperature. The minimum length that an optical probe can measure is about 20 μm. It is probable that ice crystals smaller than 20 μm could be missed by this measurement technique.

In view of the preceding discussion, the ice crystal width, mass, terminal velocity and size distribution may be parameterized in terms of the length. Using $D_{min} = 20$ μm, the bulk terminal velocity and mean effective width can be expressed as a function of the IWC, as shown in Fig. 1. In the calculations, we use a temperature range of (-30–-35°C) to obtain the coefficients A and B. Both D_e and v_T increase with increasing IWC. To investigate the effect of small ice crystals on these relationships, L_{min} in Eq. (1) is set at 10 μm and it is assumed that Eq. (4) is valid for the ice crystal size distribution that includes small ice crystals with sizes from 10 to 20 μm. The bulk terminal velocity ranges from about 1 to 10 m/s for the

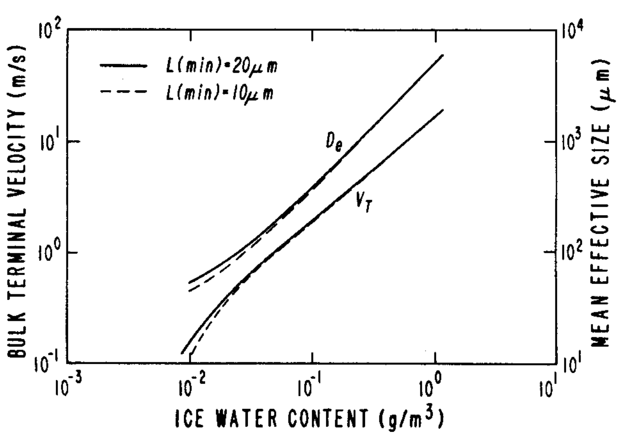

Fig. 1. Terminal velocity and mean effective size as functions of IWC

IWC from 0.1 to 1 g/m^3. For IWCs smaller than 0.1 g/m^3, the bulk terminal velocity is less than 1 m/s. The addition of ice crystals smaller than 20 μm does not affect the bulk terminal velocity significantly. Based on our present parameterizations for cloud microphysics, the mean effective size can also be theoretically computed in terms of IWC. For IWCs larger than 0.1 g/m^3, the addition of 10–20 μm sized ice crystals results in no noticeable changes in mean effective sizes. For an IWC of 0.01 g/m^3, the computed mean effective size is about 50 μm. With additional small ice crystals, this size reduces to about 40 μm. It should be emphasized that the relationship between the mean effective size and IWC that has been developed is purely theoretical and requires verification from laboratory and aircraft experiments.

Light scattering and absorption calculations require the ice crystal size distribution. However, for radiative heating and flux calculations, additional information concerning the cloud thickness and IWC is needed. It is conventional to use the optical depth to represent the optical properties of a media. The optical depth, τ, is the product of the extinction coefficient and thickness. The extinction coefficient is the product of the average extinction cross section, σ_e, and the number density of cloud particles. In the limits of geometric optics, and assuming that ice crystals are randomly oriented in space, we have $\sigma_e = 3D(\sqrt{3}/4D + L)/2$ (Takano and Liou, 1989a). This expression is derived based on the optical theorem that the extinction cross section of a large particle is twice its geometric cross section. In this case we find

$$\tau \cong (a + b/D_e) \cdot \text{IWP}, \tag{6}$$

where a and b are certain constants. For radiative transfer calculations associated with a cloud model, the two parameters defined in Eqs. (1) and (2) appear to be appropriate and sufficient.

3. Parameterization of Radiative Transfer in Clouds

For the computations of fluxes and heating rates within cloud layers, we must perform spectral integration covering the entire solar and IR spectra. These spectra may be divided into a number of spectral intervals according to the location of the gaseous absorption bands involving cloud particles and gases, primarily water vapor. In order to resolve the variation in the refractive index of ice and to account for the gaseous absorption, six and 12 bands are selected for solar and thermal IR regions, respectively. The radiative transfer methodology used is the delta-four-stream approximation developed by Liou et al. (1988). This approximation can achieve relative accuracy within about 5% for all atmospheric conditions. The solution of this approximation is in analytic form so that the computer time involved is minimal, and the method can be readily applied to inhomogeneous media by matching the continuity requirement of diffuse intensities. To apply this approximation, four expansion coefficients of the phase function are required.

The scattering and absorption properties of hexagonal ice crystals whose size parameters are greater than 30 were computed from the geometric ray-tracing technique developed by Takano and Liou (1989a, b). For size parameters that are less than 30, we used the Mie-type solution for spheroids developed by Asano and Sato (1980). Single-scattering computations were made for a number of ice crystal size distributions reported by Heymsfield and Platt (1984) and recently derived from the FIRE cirrus experiments (Heymsfield, private communication).

As pointed out previously, the optical depth may be expressed in terms of D_e and IWP, in the form given in Eq. (6), in the limits of geometric optics for scattering processes. The following general parameterization form has been derived for the spectral optical depth:

$$\tau_j = \left(\sum_{n=0}^{2} a_{n,j}/D_e^n \right) \cdot \text{IWP}, \tag{7}$$

where a_n is the known coefficient, and the subscript j (= 1,2,...,18) is the index for the spectral band. For solar wavelengths, the extinction cross sections would be the same by virtue of the geometric optical theorem. Thus, for a given thickness, Δz, the optical depth is a constant in the solar region based on the geometric ray tracing method for hexagonal ice crystals.

The single-scattering albedo is defined as: $\tilde{\omega} = 1 - \sigma_a/\sigma_e$, where σ_a and σ_e represent the absorption and extinction cross sections, respectively. In the limits of geometric optics, we have $\sigma_e = 3\,(D/2)^2(\sqrt{3} + 4L/D)/2$, as pointed out previously. The absorption cross section is generally dependent on particle volume, which is: $V = 3\sqrt{3}\,D^2\,L/8$ in the case of a hexagonal particle. Since L is related to D based on laboratory and aircraft observations, $\tilde{\omega}$ should be a function of D. Thus, it is appropriate to represent $\tilde{\omega}$ in terms of a polynomial function in the form

$$\tilde{\omega}_j = \sum_{n=0}^{3} b_{n,j} D_e^n, \tag{8}$$

where b_n is the known coefficient through numerical fittings. The third order polynomial is accurate within about 3%.

The phase function should also be a function of ice crystal size distribution, viz., the mean effective size. It follows that the expansion coefficients of the phase function may be written

$$\tilde{\omega}_{l,j} = \sum_{n=0}^{3} c_{n,l,j} D_e^n, \tag{9}$$

where the index l = 1,2,3,4 for the delta-four-stream approximation, $\tilde{\omega}_1$ = 3 g, and g is the asymmetry factor. Again, we find that the third order polynomial expansion is sufficient to provide accuracy within 3%. For solar wavelengths, the phase functions for hexagonal ice crystals show pronounced 22 and 46° halo maxima. For this reason, a simple representation using the asymmetry factor for the transfer of solar radiation in ice clouds in inadequate. However, in the thermal IR wavelengths, halo features are largely suppressed due to absorption. Thus, we may use the asymmetry factor to represent the phase function through the Henyey-Greenstein function:

$$\tilde{\omega}_l = (2l + 1) g^l. \tag{10}$$

Finally, to incorporate the forward peak contribution in multiple scattering, we may use the similarity principle for radiative transfer to adjust the optical depth, single-scattering albedo and phase function in the forms (Liou et al., 1988)

$$\tau' = \tau(1 - f\tilde{\omega}), \tag{11 a}$$

$$\tilde{\omega}' = (1 - f)\tilde{\omega}/(1 - f\tilde{\omega}), \tag{11 b}$$

$$\tilde{\omega}'_l = [\tilde{\omega}_l - f(2l + 1)]/(1 - f), \tag{11 c}$$

where the fraction of scattered energy residing in the forward peak, $f = \tilde{\omega}_4/4$. The wavelength index j has been omitted in these equations.

Using the preceding parameterizations for cloud physics and radiative transfer, Fig. 2 shows solar reflectance and absorptance and IR emittance (or emissivity) as functions of D_e and IWP. A cosine of the solar zenith angle of 0.5 is used in solar radiative transfer calculations. For a given D_e, solar reflectance increases with increasing IWP. But for a given IWP, a cloud with a smaller D_e reflects more solar radiation because of the larger effective cross section area. For example, for an IWP of 100 g m^{-2}, solar reflectances of

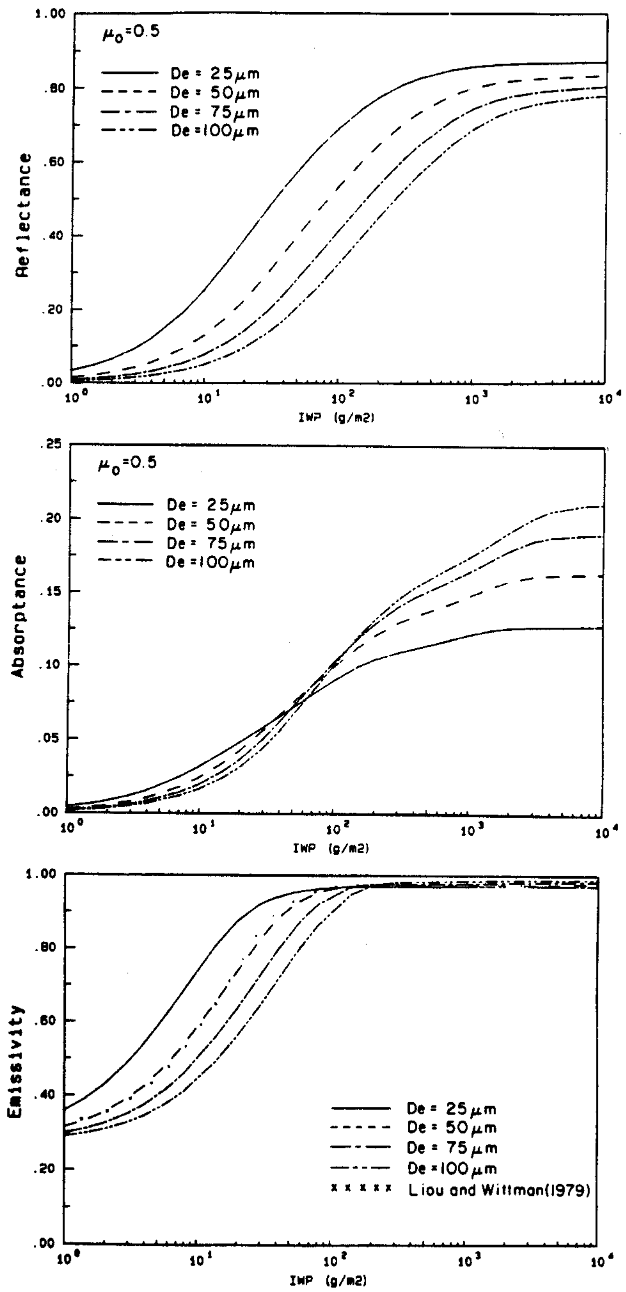

Fig. 2. Solar reflectance and absorptance and IR emittance (or emissivity) as functions of the mean effective size and ice water path

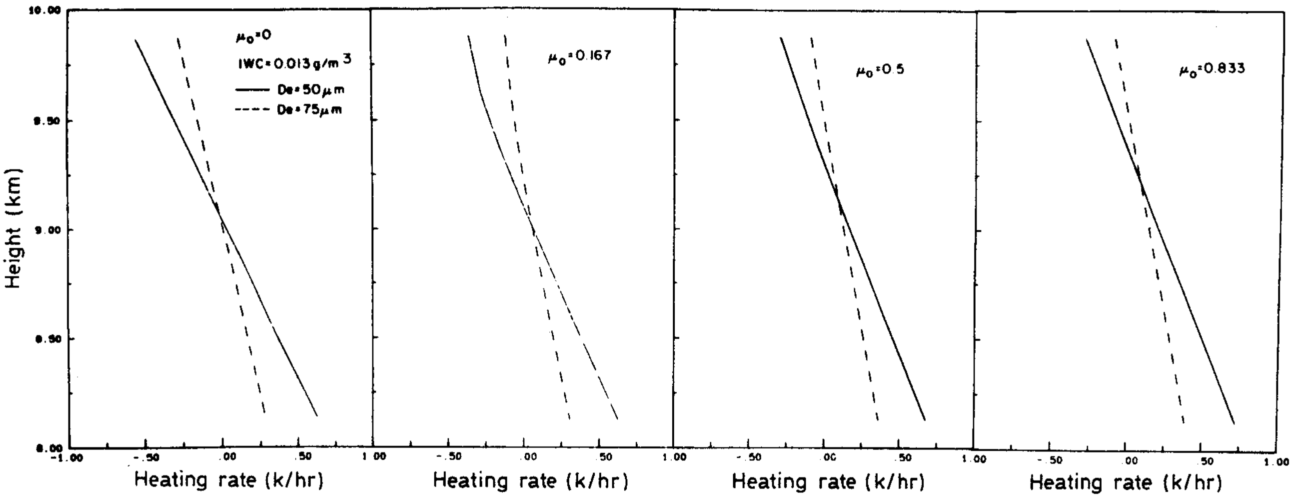

Fig. 3. Net radiative heating rates as functions of height and cosines of the solar zenith angle, μ_o, for mean effective sizes of 50 and 75 μm

about 70, 55, 44 and 30% are shown for D_e of 25, 50, 75 and 100 μm, respectively. For solar absorptance, small ice crystals also absorb more solar radiation for IWPs up to 75 g m^{-2}. However, absorption of solar radiation also depends on forward scattering of cloud particles. Larger particles would have stronger forward scattering and absorb more solar radiation when the IWP is larger than about 75 g m^{-2}. The IR emissivity is significantly dependent on both D_e and IWP. For a given IWP of 20 g m^{-2}, emissivity differs by as much as 40% for D_e of 25 and 100 μm.

The effects of the ice crystal mean effective size on net radiative heating are illustrated in Fig. 3. In the calculations, we use an IWP of 26 g m^{-2}, which corresponds to an IWC of 0.013 g m^{-3} for a typical cirrostratus with a thickness of 2 km. This cloud is inserted in the standard atmospheric temperature and humidity profiles. A solar constant of 1365 W m^{-2} and a surface albedo of 0.1 are used in the solar radiation calculation. The optical depths for D_e of 50 and 75 μm are approximately 2 and 1, respectively. Net radiative heating rates that correspond to four cosines of the solar zenith angle of 0, 0.167, 0.5 and 0.833 are displayed in Fig. 3. When $\mu_o = 0$, only IR heating/cooling takes place. In this case, a smaller D_e of 50 μm produces heating/cooling rates of about 0.6–0.7°C h^{-1} close to the bottom and top of the cloud layer. For a D_e of 75 μm, the heating/cooling rates at the cloud bottom and top reduce by as much as a factor of two. This reduction is due to the fact that a cloud having smaller D_es emits more IR radiation at the colder cloud top. The cloud absorbs, at the same time, more IR radiation emitted from the warmer surface and atmosphere below, resulting in strong heating at the cloud base region. The solar heating rate increases with decreasing D_e and occurs primarily at the cloud top, where IR cooling is much more pronounced. For $\mu_o = 0.833$, the solar heating rate is a factor of about three smaller than the IR cooling rate at the cloud top. It is evident from this illustration that the cloud field is largely controlled by IR heating/cooling and that the presence of small ice crystals may generate a steeper lapse rate within clouds.

4. The Role of the Mean Effective Cloud Particle Size in Large-Scale Cloud Processes

To investigate the sensitivity of cloud microphysics and radiative transfer parameterizations to large-scale cloud processes, the 3-D global cloud model developed by Lee et al. (1990) is used. This cloud model consists of thermodynamic equations for the prediction of water vapor, cloud liquid water content (LWC) and IWC, precipitation and temperature. However, the wind field is prescribed using the results from a general circulation model (GCM). The model has a 12-layer stretch vertical coordinate, which has a fine resolution in the lower levels. Cloud covers are computed from the threshold method. To compare with the observed cloud fields and to perform radiative transfer calculations, the model generated cloud parameters are strapped into low, middle and high clouds. The cloud microphysical processes considered in the model are evaporation, condensation, autoconversion, sublimation/deposition, homogeneous nucleation, Bergeron processes, and gravitational setting for ice crystals. As described in Section 2, the gravitational setting is parameterized in terms of the bulk terminal velocity, which is critical to the simulation of IWC. Radiative transfer parameterizations for clouds follow those presented in Section 3. In particular, two cloud parameters, i.e., the mean effective size and IWP, are incorporated in radiation calculations. The analysis data for winds, temperature, and specific humidity at 12Z 1 July 1979 are used as initial values to perform the large-scale prediction for cloud fields.

We shall confine our discussion to the effects of the mean effective size of ice crystals on large-scale cloud simulations. The interactions and feedbacks of cloud microphysics, radiative transfer, and the cloud model are shown in Fig. 4. The model predicts IWC (and LWC), cloud cover, temperature, and specific humidity. The bulk terminal velocity and mean effective size are defined based on the cloud microphysics parameterizations. The IWC together with the model thickness give the IWP. The terminal velocity is directly related to IWC by means of parameterization and is interactive in the cloud model. Although we have developed a theoretical relationship between IWC and D_e, this relationship has yet to be verified. In this study, we shall treat D_e and IWP as two independent parameters to investigate the sensitivity

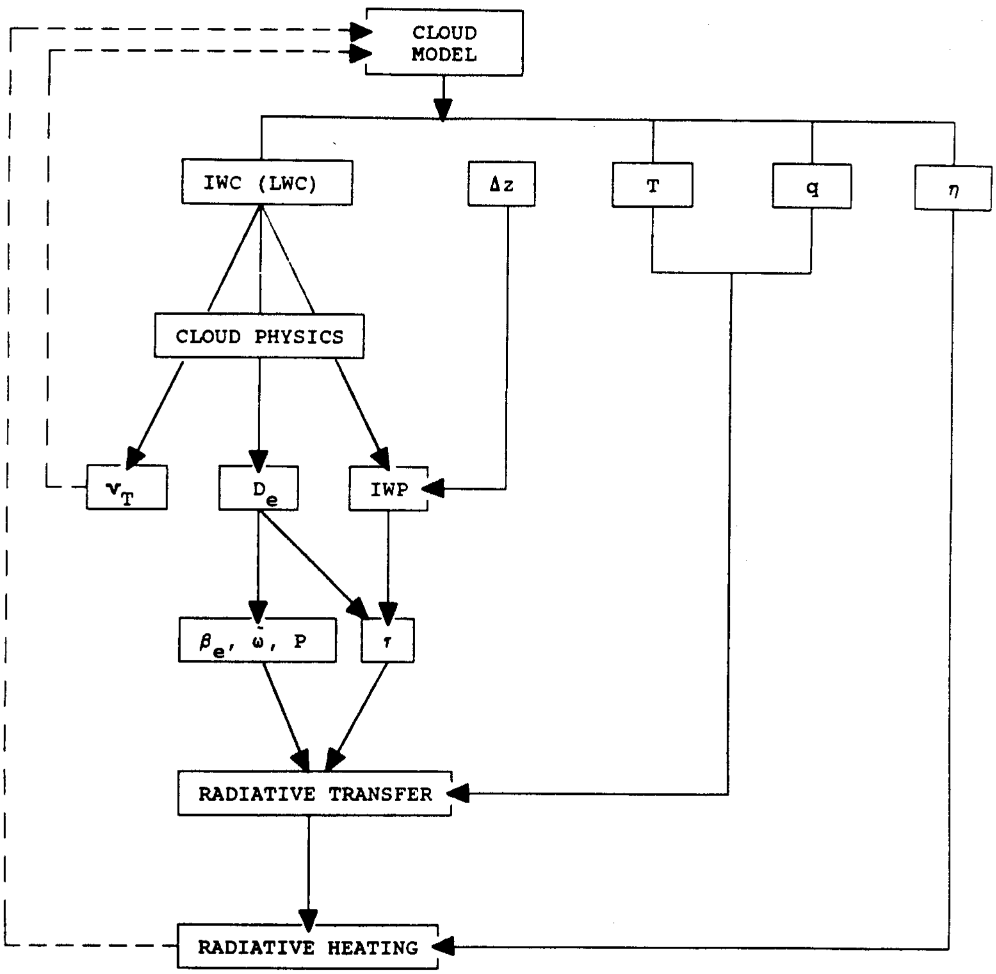

Fig. 4. Interactions and feedbacks of cloud microphysics, radiative transfer and the cloud model. In this diagram, η denotes cloud cover, V_T is the bulk terminal velocity, D_e is the mean effective size, β_e is the extinction coefficient, $\tilde{\omega}$ is the single-scattering albedo, P is the phase function, τ is the optical depth, T is temperature and q is the specific humidity

of D_e on the simulations of large-scale cloud fields. Light scattering and absorption calculations for cloud particles require only information on particle size distribution, which is parameterized in terms of D_e. For radiative transfer calculations, the optical depth value is also needed. As shown in the preceding sections, the optical depth can be expressed in terms of D_e and IWP. Temperature and humidity are inputs in radiative transfer calculations. Lastly, cloud cover from the model is required to compute the average radiative heating in a model grid area. Radiative heating affects temperature directly via the thermodynamic heat equation, while the bulk terminal velocity affects IWC (and LWC) directly through the governing equations for IWC, LWC and precipitation.

Comparisons of the zonally averaged total cloud cover and outgoing longwave radiation (OLR) predicted from the model and derived from observations are shown in Figs. 5a and 5b. The

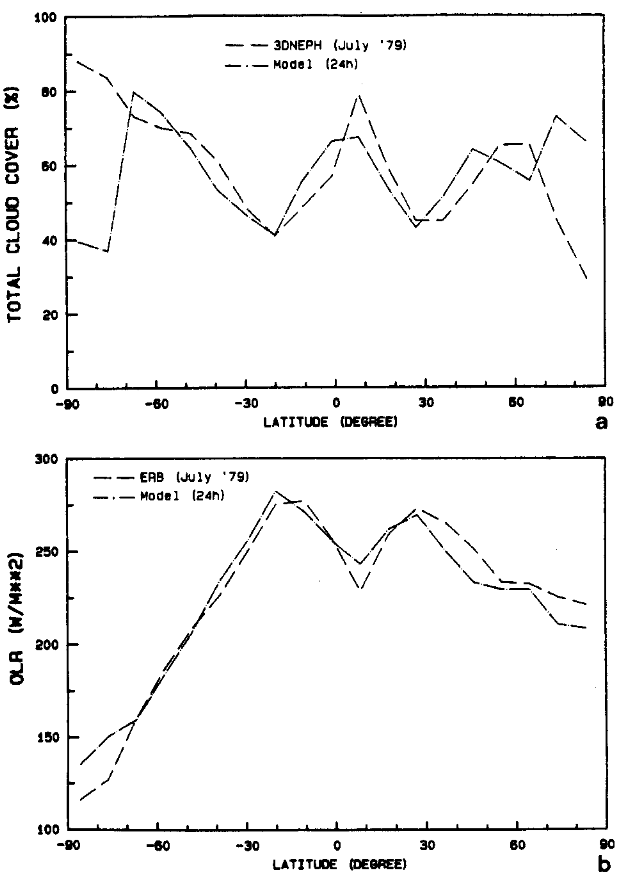

Fig. 5. Comparisons of the zonally averaged (a) total cloud cover and (b) OLR predicted from the model and derived from 3DNEPH and ERB for July 1979. The model results are for averages over a 24 h period

predicted cloud covers are averages of the results computed at 96 time steps over a 24 hour period. The observed cloud covers are taken from Henderson-Sellers (1986) based on the 3DNEPH data base for July 1979. It is well known that the 3DNEPH under- and over-estimates cloud cover in Arctic and Antarctic regions, respectively, for the summer season of the Northern Hemisphere. During this period, there are persistent stratus clouds over the Arctic region. However, the threshold method utilized in 3DNEPH has not been able to distinguish between the cold surface and clouds aloft. As a result, because of cold temperatures in the Antarctic region during the northern summer, the threshold technique overestimates cloud cover. The model underestimates cloud cover in the tropics because of the nature of the present 3-D global cloud model, which was developed primarily for stratiform clouds. It appears that improvements could be made if a cumulus convection program were added in the model. Nevertheless, there are general similarities between the predicted and observed cloud covers. The OLR fields computed from the model compare reasonably well with the monthly averaged data from ERB for July 1979. Discrepancies between the two may be explained by the cloud cover patterns described previously. In summary, the similarities between the model results and observations in terms of cloud cover and OLR are encouraging in view of the simplicity of the cloud model structure. Sensitivity experiments are carried out to investigate the relative importance of the mean effective size on the predicted large-scale cloud field.

The cloud model predicts IWC for high clouds and LWCs for middle and low clouds. Mean effective sizes of 50 and 75 μm are used in large-scale cloud simulations. The value of 50 μm corresponds to the mean effective size for a typical cirrostratus. Shown in Figs. 6a, 6b and 6c are the zonally averaged differences in the IR, solar and net heating rates predicted by the model for a 24 hour period. For smaller D_e, the IR emissivity is greater for high clouds, leading to more cooling at high cloud tops. However, the greater high cloud emissivity produces heating at high cloud bases and increases heating rates in the middle cloud level. The contour lines in Fig. 6a are for each 0.3°C day^{-1}. The increase of high cloud top cooling for smaller D_e is on the order of about

0.3°C day^{-1} in cloud regions. In the middle cloud level, heating rates increase by about 0.6°C day^{-1}. These values are significant, since they are zonally averaged quantities. No change is seen in the heating rate patterns below middle clouds. The differences in solar heating rates produced by the two mean effective sizes are confined in the Northern Hemisphere because the July condition is used. A smaller D_e reflects more solar radiation and increases solar heating in high cloud top regions. At the same time, it reduces the solar fluxes available in the middle cloud level. The contour lines in Fig. 6b are for each 0.02°C day^{-1}, which is 15 times smaller than the IR heating/cooling rates. Figure 6c shows the net heating differences. The patterns are similar to the IR heating/cooling patterns. The exception is the reduction of cooling above high cloud top regions in the Northern Hemisphere.

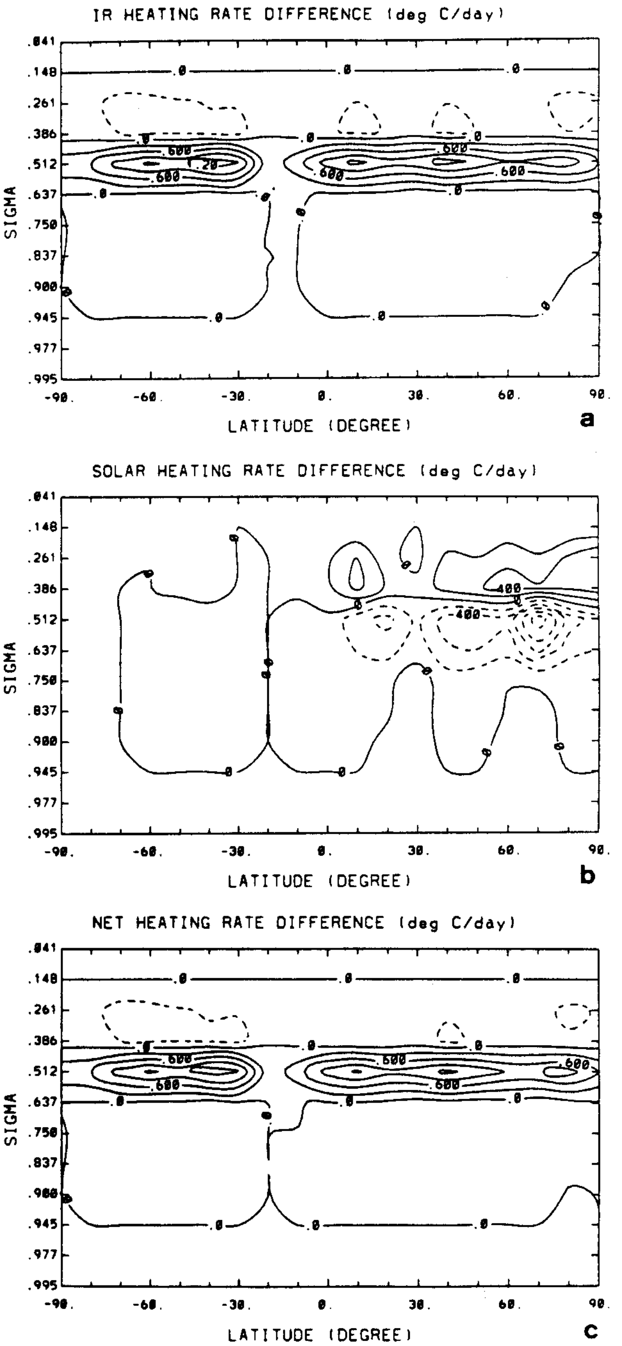

Fig. 6. Zonally averaged differences in (a) IR, (b) solar and (c) net heating rates for a 24 h period using mean effective sizes of 50 and 75 μm in numerical experiments

Figures 7a–7c show the effects of the mean effective size on the simulation of temperature, cloud cover and IWC. Because of more cooling produced by a smaller D_e above the high cloud top, temperatures decrease there (Fig. 7a). The maximum decrease is on the order of about 0.2–0.4°C. However, temperature increases in the middle cloud level by about 0.4°C across the latitudes. In response to temperature decreases above the high cloud top, high cloud cover increases. The increase of high cloud cover is on the order of 4% across most latitudes (Fig. 7b). The use of different mean effective sizes of ice crystals significantly affects the calculation of middle cloud cover due to temperature increases. Except in the vicinity of 30°S where the occurrence of clouds is minimal, middle cloud cover is reduced by 3 to 4% between 60°N and 60°S latitudes because of warmer temperatures produced by IR heating. In terms of IWC for high clouds (Fig. 7c), differences produced by the two simulations are rather small because IWC is largely controlled by the bulk terminal velocity, which is interactive in the model. Variations in the mean effective size do not affect the bulk terminal velocity in the present experiments. It appears that IWC variations are primarily governed by microphysical processes. If the mean effective size could be made interactive through IWC, radiative perturbations would be important in the generation of IWC.

The preceding experiments have been carried out to explore the importance of the mean effective size of ice crystals in large-scale cloud simulations. Based on experimental results, small mean effective size, through radiative heating perturbations, would increase high cloud cover and, at the same time, reduce middle cloud cover. It is commonly recognized that the prime importance of high clouds is the downward emission of IR radiation

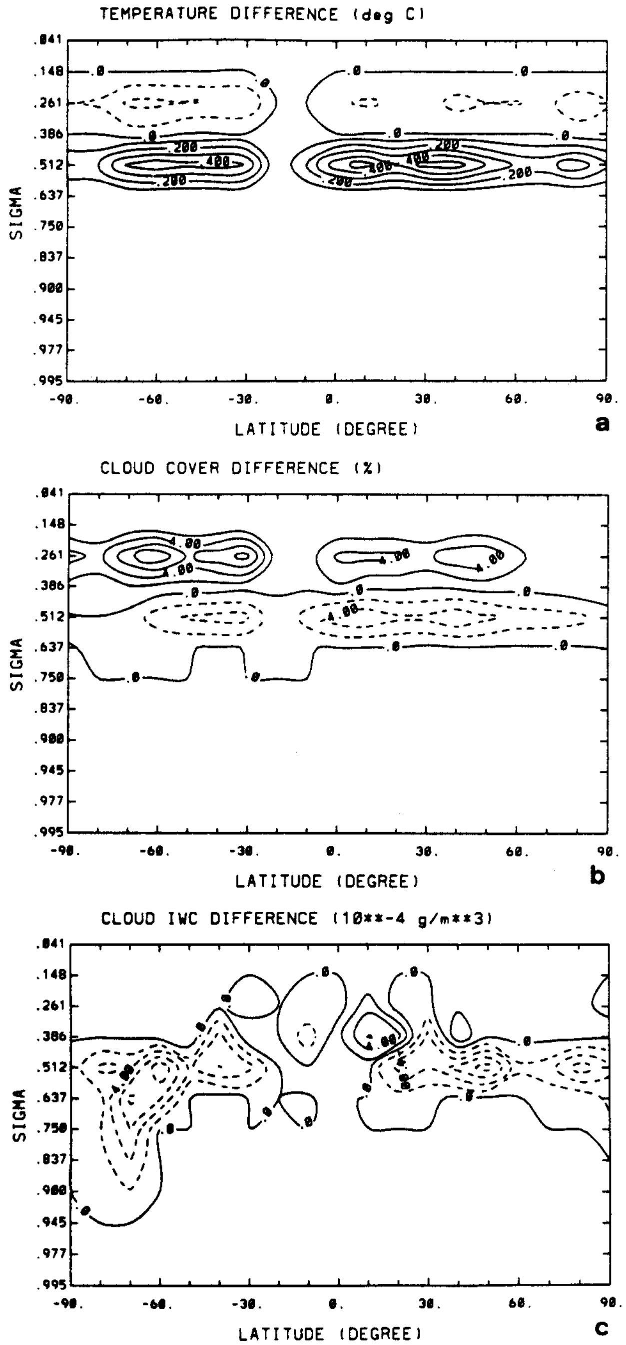

Fig. 7. Zonally averaged differences in (a) temperature, (b) cloud cover and (c) cloud IWC for a 24 h period using mean effective sizes of 50 and 75 μm in numerical experiments

(greenhouse effect). For middle clouds, it is the reflection of solar radiation (solar albedo effect). The increase of high cloud cover and the decrease of middle cloud cover would lead to the amplification of the greenhouse effect. Small mean effective sizes are normally considered to be significant in the reflection of sunlight. However, we have demonstrated in this study that the prevailing effects of small mean effective sizes are in the production of IR heating and cooling. The IR heating and cooling in the atmosphere produced by small mean effective sizes are much more significant than the solar heating counterpart.

5. Conclusions

Parameterization programs for cloud microphysics and radiative transfer involving ice clouds have been developed in conjunction with a 3-D global cloud model. We show that the mean effective size and IWP are two variables that are related to the optical depth. The mean effective size appears sufficient to define the ice crystal size distribution with respect to light scattering and absorption calculations. We illustrate the importance of the mean effective size in radiative transfer calculations in terms of solar reflectivity, IR emissivity and radiative heating. For a given IWP, smaller mean effective sizes reflect more solar radiation, emit more IR radiation and enhance net radiative heating/cooling at the cloud top and bottom than larger sizes.

A 3-D global cloud model has been used to investigate the effects of the mean effective size of ice crystals on the simulation of cloud cover and IWC. This model has been verified through comparisons of the predicted cloud cover and OLR with monthly averaged values derived from 3DNEPH amd ERB. High clouds that are composed of smaller mean effective sizes would produce more cooling at the cloud top and more heating at the cloud base, than high clouds composed of larger sizes. As a result of these heating/cooling patterns, more high cloud cover and less middle cloud cover are simulated from the model. Using the mean effective sizes of 50 and 75 μm, a ~ 4% increase and 3–4% decrease are shown for high and middle cloud covers, respectively. The radiative heating/cooling patterns, however, do not affect IWC for high clouds or LWC for middle clouds because the mean effective size is prescribed in the model. If a relationship could be established between the mean effective size and IWC, radiative heating through the mean effective size would influence the prediction of IWC as well as LWC for middle clouds.

On the basis of the preceding discussion, it would be important to develop a relationship between the mean effective size of ice crystals and IWC from aircraft experimental data. Second, radiative transfer parameterizations that encompass the mean effective size developed in Section 3 should be verified through concurrent radiation and cloud microphysics experiments involving ice clouds. Finally, the 3-D global cloud model may be improved by incorporating time varying wind fields to study their effects on the simulations of cloud parameters in the context of cloud microphysics/radiative transfer parameterizations. The program may be accomplished by using a separate and parallel GCM to produce the required wind fields.

Acknowledgements

This research has been supported by the Air Force Office of Scientific Research Grant AFOSR87-0294, NSF Grant ATM88-15712 and NASA Grant NAG5-1050. We thank Professors H. Sundqvist and L. Donner for helpful comments on this paper.

References

Asano, S., Sato, M., 1980: Light scattering by randomly oriented spheroidal particles. *Appl Opt.*, **19**, 962–974.

Auer, A. H., Jr., Veal, D. L., 1970: The dimension of ice crystals in natural clouds. *J. Atmos. Sci.*, **29**, 919–926.

Henderson-Sellers, A., 1986: Layered cloud amounts for January and July, 1979 from 3-D Nephanalysis. *J. Climate Appl. Meteor.*, **25**, 118–132.

Heymsfield, A. J., 1972: Ice crystal terminal velocities. *J. Atmos. Sci.*, **29**, 1348–1357.

Heymsfield, A. J., 1977: Precipitation development in stratiform ice clouds: A microphysical and dynamical study. *J. Atmos. Sci.*, **34**, 367–381.

Heymsfield, A. J., Platt, C. M. R., 1984: A parameterization of the particle size spectrum of ice clouds in terms of the ambient temperature and the ice water content. *J. Atmos. Sci.*, **41**, 846–856.

Heymsfield, A. J., Donner, L. J., 1990: A scheme for parameterizing ice-cloud water content in general circulation models. *J. Atmos. Sci.*, **47**, 1865–1877.

Hobbs, P. V., Chang, S., Locatelli, J. D., 1974: The dimensions and aggregation of ice particles in natural clouds. *J. Geophys. Res.*, **79**, 2199–2206.

Jayaweera, K., Cottis, R. E., 1969: The fall velocities of plate-like and columnar ice crystals. *Quart. J. Roy. Meteor. Soc.*, **95**, 703–709.

Lee, J. L., Ou, S. C., Liou, K. N., 1990: The effects of ice processes and infrared cooling on the formation of high clouds in a 3-D global cloud model. Preprint, *The Seventh Atmospheric Radiation Conference*, San Francisco, July 23–27, American Meteorological Society, Boston.

Liou, K. N., Zheng, Q., 1984: A numerical experiment on the interactions of radiation clouds and dynamic processes in a general circulation model. *J. Atmos. Sci.*, **41**, 1513–1535.

Liou, K. N., Fu, Q., Ackerman, T. P., 1988: A simple formulation of the delta-four-stream approximation for radiative transfer parameterizations. *J. Atmos. Sci.*, **45**, 1940–1947.

Smith, R. N. B., 1990: A scheme for predicting layer clouds and their water content in a general circulation model. *Quart. J. Roy. Meteor. Soc.*, **116**, 435–460.

Starr, D. C., Cox, S. K., 1985: Cirrus clouds. Part I: A cirrus cloud model. *J. Atmos. Sci.*, **42**, 2663–2694.

Sundqvist, H., 1988: Parameterization of condensation and associated clouds in models for weather prediction and general circulation simulation. In: Schlesinger, M.E., (ed), *Physically-Based Modelling and Simulation of Climate and Climate Change*, Reidel, pp 433–461.

Takano, Y., Liou, K. N., 1989a: Radiative transfer in cirrus clouds. I. Single-scattering and optical properties of hexagonal ice crystals. *J. Atmos. Sci.*, **46**, 3–19.

Takano, Y., Liou, K. N., 1989b: Radiative transfer in cirrus clouds. II. Theory and computation of multiple scattering in an anisotropic medium. *J. Atmos. Sci.*, **46**, 20–36.

Authors' address: Prof. K. N. Liou, J. L. Lee, S. C. Ou, Q. Fu and Y. Takano, University of Utah, Department of Meteorology/CARSS, Salt Lake City, Utah 84112, U.S.A.